

Seismic Response in Catania by Different Methodologies

S. Grasso⁽¹⁾, G. Laurenzano^(2,3), M. Maugeri⁽¹⁾ and E. Priolo⁽²⁾

(1) Dipartimento di Ingegneria Civile e Ambientale, Università di Catania

(2) Istituto Nazionale di Oceanografia e di Geofisica Sperimentale (OGS), Trieste

(3) Dipartimento di Ingegneria Civile, Università degli Studi di Trieste

Abstract

The prediction of the seismic response and assessment of the amplification factor of the surface soils is a topic of maximum interest in engineering seismology and the final goal of any microzonation study. Two very different numerical techniques, are employed in this paper. One is a 2-D method, the Spectral Element Method (SPEM-2D), which solves the propagation of the seismic field through complex geological structures. The other is a 1-D method (by the GEODIN code), commonly used in engineering practice, which takes into account the detailed shear waves soil profile of superficial layers, including soil non-linearity. The seismic response at the surface by 1-D code is evaluated, using as input motion at the conventional bedrock scaled recorded accelerograms and synthetic accelerograms given by the 2-D code at a given depth. A comparison between soil response at the surface, given by the 2-D method and by the 1-D method is presented. In particular the effects of the seismic input, of the shear waves soil profile and of the soil non-linearity, are analysed and discussed.

1 Introduction

The prediction of the seismic response and assessment of the amplification factor of the surface soils is a topic of maximum interest in engineering seismology and the final goal of any microzonation study. In this study, we compare the results

obtained using two different methods of numerical modelling of seismic wave propagation to assess the seismic response at seven sites in Catania.

One is a 2-D method (the spectral element method (SPEM-2D) which solves the propagation of the seismic field through complex geological structures and permits estimation the effects of deep crustal structure, superficial geology and irregular topography on the ground shaking. By this method, synthetic accelerograms can be evaluated at the surface but also at a given depth and in particular at the conventional bedrock. The other is a 1-D method, which is commonly used in engineering practice. According to Eurocode 8 [1] the hazard is described in terms of effective peak ground acceleration in rock or firm soil (i.e. conventional bedrock). 1-D methods are used for evaluation of the site amplification in the upper 30 m of soil. To evaluate the seismic response at the surface, the seismic input motion at the conventional bedrock is then needed. In this paper, as input motion, we have used scaled recorded accelerograms and synthetic accelerograms given by the 2-D code at a given depth.

One of the goals of the paper is to estimate the range of applicability of classical 1-D methods, compared to more sophisticated 2-D techniques. By 1-D models it is not possible to take into account the effects of the irregular topography on the ground shaking, but it is more easy to take into account the effects of the detailed shear waves soil profile and of the soil non-linearity.

2 SPEM 2-D simulation

The Chebyshev spectral element method SPEM 2-D solves propagation of the seismic field through complex geological structures and enables one to estimate the effects of deep crustal structure, superficial geology and irregular topography on the ground shaking. The following approach solves the full wave field, including converted body waves and surface waves and allows for an accurate description of the medium heterogeneity at several scale lengths. In this way the ground motion induced not only by the uppermost soil layers but also by the deep interfaces is reproduced with high accuracy. Numerical simulations are performed along 2-D vertical planes containing both source and receivers. More details about SPEM and its application to the solution of the seismic waves equations can be found in Seriani and Priolo [2], Priolo [3] and in Priolo [4]. The source of the reference event for this study is located along the northern part of the Ibleo-Maltese fault and has a purely normal mechanism (Figure 1).

This fault is indicated as the probable source of the $M \approx 7$ earthquake, which struck the city of Catania in 1693 (Postpischl [5]). The computational domain in which the wavefield is modelled is a vertical plane extending approximately 32 km in length and 20 km in depth. The extended source consists of the summation of 5 subevents, which reproduce approximately the rupture propagation along the fault segment and the heterogeneous distribution of the seismic moment along the fault. The different seismic moment distributions are shown in a schematic way in Figure 2 for the position of the five “elementary” point sources shown in Figure 3 (bottom panel).

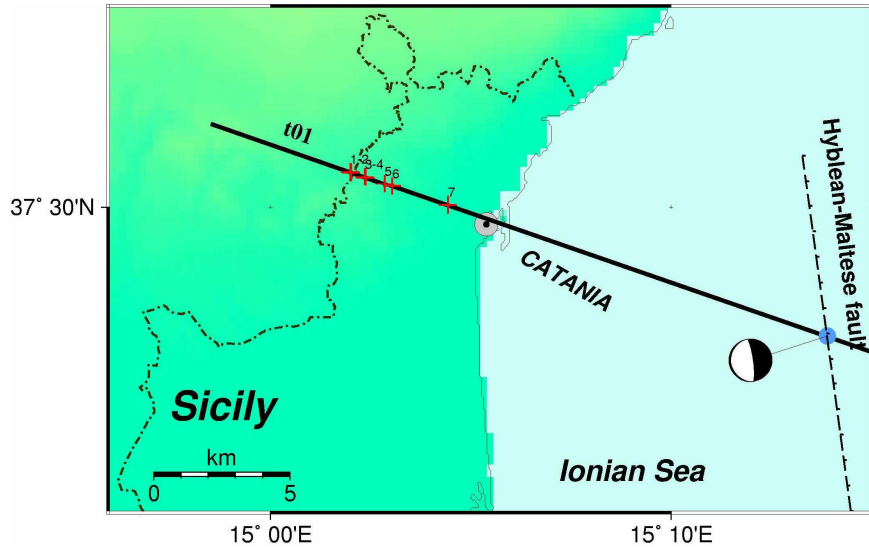


Figure 1. Base map of the study area, showing the transect position and the site locations. The circle shows the assumed position of the reference earthquake of January 11, 1693.

The corner frequency of each time history is equal to 0.24 Hz, corresponding to the asperity (Heaton [6]). The amplitude of the computed wave field is scaled by the average value of the slip (or dislocation) at the source. Following the scaling laws, this value has been estimated as $D = 1.34$ metres (Wells and Coppersmith [7]; Sommerville *et al.* [8]). The seismograms have been computed up to a maximum frequency of 8 Hz.

The structural model is characterized by a carbonatic basement (Cc), overlapped by sedimentary units of volcanic and alluvial origin (Figure 3 and Table 1). Rock formations and soils are expressed in terms of body wave velocities, density and attenuation (through the quality factor). The elastic behaviour of the rocks is assumed to be linear and isotropic. The shallowest part of the model has been constructed in detail using all the available geological, geophysical and geotechnical information. Table 2 shows the shear wave velocities of the shallowest layers at the sites where the seismic response is evaluated. Seismograms have been computed at each site for six receivers located at increasing depths from the surface to about 170 metres deep.

Four different distributions and release of the seismic moment have been simulated at the source. As an example, the waveforms (accelerations) computed for receiver n.1 and for the seismic moment distribution IBM_A are shown in Figure 4. The largest peak accelerations have been obtained for the moment distribution model called IBM_B, followed by IBM_D, IBM_C and IBM_A.

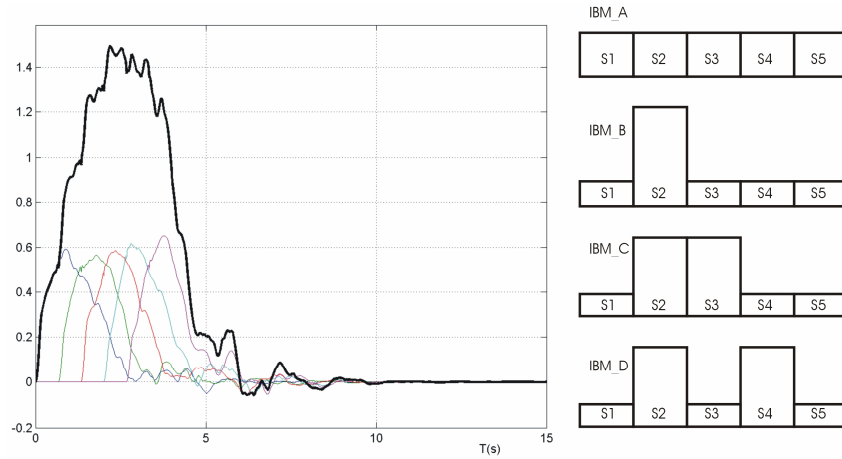


Figure 2. Left panel: source time history. The coloured lines indicate the five source time functions, located at different depth (points S1-S5 in Figure 4, bottom panel). The black line is the sum of the five functions. In this example the seismic moment distribution is homogeneous (model IBM_A in the right panel). Right panel: seismic moment distributions. From top to bottom: uniform moment distribution (IBM_A), one-asperity models (IBM_B and IBM_C) and two-asperities model (IBM_D).

Table 1. Description of the main soil and rock formations used to define the transect.

| Material description | Id |
|---|------------------|
| Clays and silt, interbedded with sand | ASg |
| Silty clays and grey-bluish marly clays | Aa ₁ |
| | Aa ₂ |
| Fine alluvial deposits | Alf |
| Coarse alluvial deposits | Alg |
| Marine deposits | M |
| Top soil and fill | R _# |
| Sands, sandstones and conglomerates | SG _# |
| Pliocenic sediments and alloctonous | Spa _# |
| Scoriaceous lavas, lavas in blocks | X |
| Lava flows | E |
| Vulcanits | V |
| Limestone (carbonatic basement) | Cc _# |

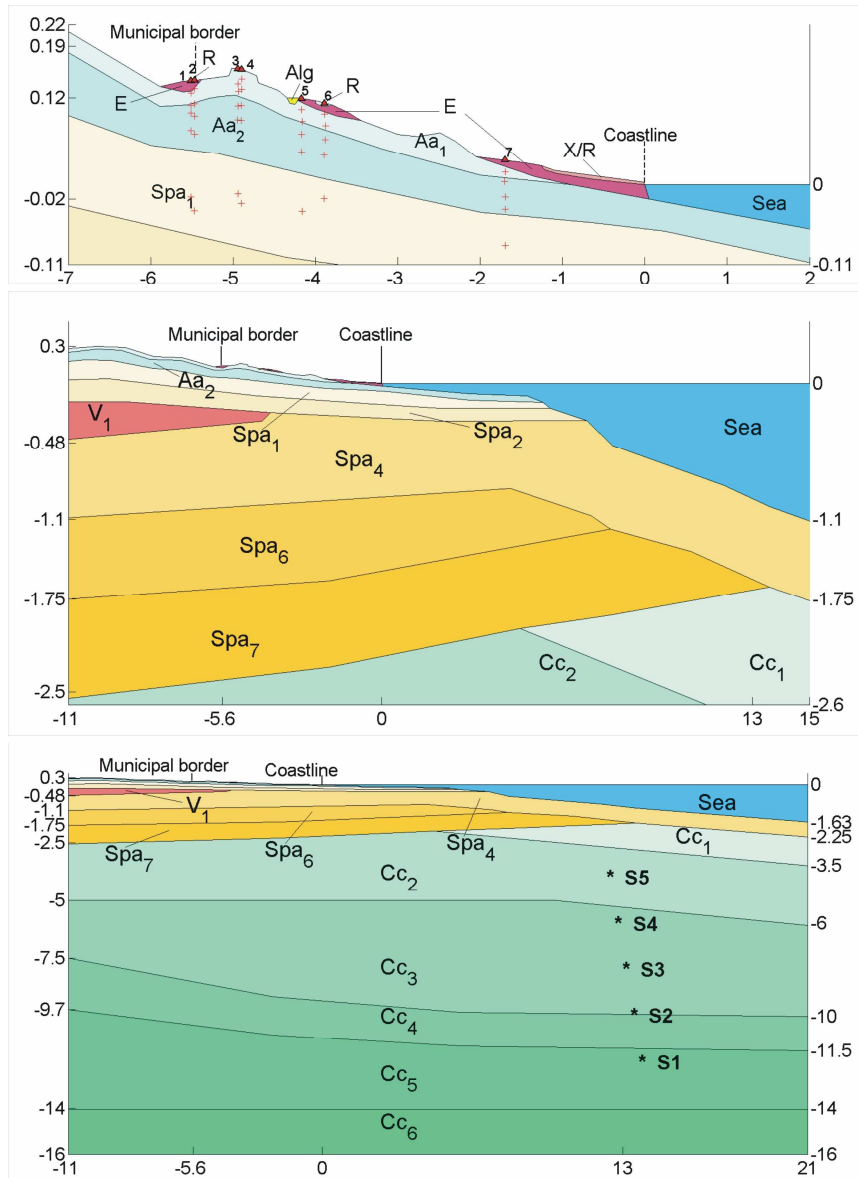


Figure 3. Structural model of the transect at different levels of detail. In the top panel are indicated the location of the seven study sites (triangles on the surface) and the location, at growing depth, of the other “receivers”, where the seismograms have been extracted.

Table 2. Description of the main properties of the sites.

| | Soil formation | Thickness (m) | V_s (m/s) |
|--------|----------------|---------------|-------------|
| Site 1 | R | 6 | 600 |
| | E | 7 | 1000 |
| | Aa | 83 | 250-500 |
| | Spa | - | 775 |
| Site 2 | R | 4 | 250 |
| | E | 5 | 900 |
| | Aa | 86 | 250-500 |
| | Spa | - | 775 |
| Site 3 | Aa | 123 | 250-500 |
| | Spa | - | 775 |
| Site 4 | Aa | 123 | 250-500 |
| | Spa | - | 775 |
| Site 5 | E | 7 | 1000 |
| | Aa | 96 | 250-500 |
| | Spa | - | 775 |
| Site 6 | R | 5 | 250 |
| | E | 8 | 1000 |
| | Aa | 91 | 250-500 |
| | Spa | - | 775 |
| Site 7 | E | 9 | 1000 |
| | Aa | 67 | 250-500 |
| | Spa | - | 775 |

3 1-D simulation

The 1-D simulation is made by the GEODIN code [9], which is commonly used in engineering practice. The GEODIN implements a one-dimensional simplified, hysteretic model for the non-linear soil response. The model (Maugeri and Frenna [10]) has been validated by means of some experiments (Maugeri *et al.* [11]). The S-wave propagation occurs on a 1-D column having shear behaviour. The column is subdivided in several horizontal, homogeneous and isotropic layers characterized by a non-linear spring stiffness $G(\gamma)$, a dashpot damping $D(\gamma)$ and a soil mass ρ . Moreover, to take into account the soil non-linearity, laws of shear modulus and damping ratio against strain can be inserted in the code.

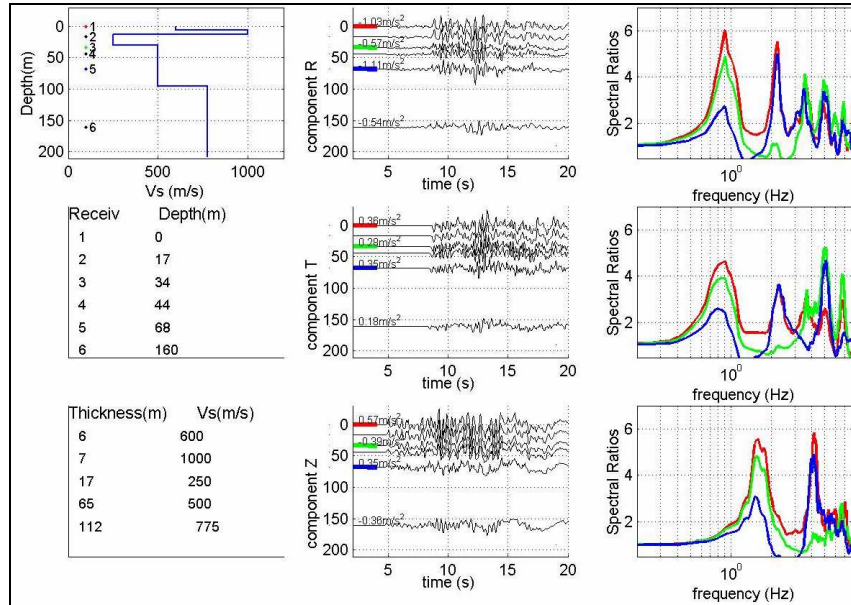


Figure 4. Model IBM_A, site n. 1. Left, top panel: seismic velocity profile. Receiver position and number are explicitly indicated. Left, central panel: receiver depth. Left, bottom panel: thickness and shear wave velocity of each layer. Central panels: accelerograms computed for the three components: radial (top), transversal (centre) and vertical (bottom). Right panels: ratios between the amplitude spectra of the receivers called 1 (red colour), 3 (green) and 5 (blue) respectively, and the receiver 6 located at the bottom ($z \sim 170$ m).

According to Eurocode 8 [1] the hazard is described in terms of effective peak ground acceleration in rock or firm soil (i.e. conventional bedrock). The 1-D method is used for evaluation of the site amplification in the upper 30 m of soil. To evaluate the seismic response at the surface, the seismic input motion at the conventional bedrock is then needed. In this paper, as input motion, we have used scaled recorded accelerograms of the December 13, 1990 eastern Sicily earthquake. In particular the recorded accelerograms at the stations of Sortino (rock soil) and Catania (soft soil) (Rovelli *et al.* [12]) are used. As the largest peak acceleration has been obtained for the moment distribution called IBM_B, synthetic accelerograms for this moment distribution, at a depth of 30 m (i.e. conventional bedrock) are also used as input accelerograms.

The input motions are evaluated for soil stratigraphy given in Table 2, where the main soil properties are listed. More details are given by boreholes located near to each site. In Table 3 for each site are given the corresponding boreholes, the locations of boreholes, the elevation, the depth and the Gauss-Boaga coordinates. Soil non-linearity is taken into account by the following expressions:

$$\frac{G(\gamma)}{G_0} = \frac{1}{1 + \alpha\gamma(\%)^\beta} \quad (1)$$

$$D(\gamma)(\%) = \eta \cdot \exp\left[-\lambda \cdot \frac{G(\gamma)}{G_0}\right] \quad (2)$$

in which: G_0 = initial shear modulus; $G(\gamma)$ = strain dependent shear modulus; γ = shear strain; α , β = soil constants; $D(\gamma)$ = strain dependent damping ratio; η , λ = soil constants. For soft soil at the site of via Stellata (Maugeri and Cavallaro [13]), the values are: $\alpha = 11$, $\beta = 1.119$, $\eta = 31$, $\lambda = 1.921$. For stiff soil at the site of San Nicola alla Rena Church (Cavallaro *et al.* [14]), the values are: $\alpha = 7.5$, $\beta = 0.897$, $\eta = 90$, $\lambda = 4.5$.

Table 3. Borehole locations near each site of Table 2.

| | Borehole | Locality | Elev. (m) | Depth (m) | Longitude | Latitude |
|--------|----------|------------------|-----------|-----------|-----------|----------|
| Site 1 | 1068 | Misterbianco | 143 | 10 | 2522870 | 4151590 |
| Site 2 | 1069 | Misterbianco | 143 | 11.7 | 2522920 | 4151600 |
| Site 3 | 408 | M.te Po S. Media | 155 | 18 | 2523428 | 4151438 |
| Site 4 | 409 | M.te Po S. Media | 155 | 18 | 2523449 | 4151432 |
| Site 5 | 130 | Via Monte Po | 118 | 8 | 2524141 | 4151118 |
| Site 6 | 131 | Piazza Ungheria | 112 | 8 | 2524454 | 4151123 |
| Site 7 | 1427 | Piazza Palestro | 37.5 | 40 | 2527131 | 4151272 |
| | 346 | Piazza Palestro | 37.5 | 30.7 | 2526492 | 4150296 |

By way of an example, the soil response at site No. 3 of Figure 3 is reported. The main soil properties at the site are reported in Table 2, while more details are given by borehole No. 408 located near to site No. 3. Detailed soil properties given by borehole No. 408 are reported in Table 4. From Table 4 it is possible to see the presence of layers of fine alluvial deposits and silty clay alternatively, ignored by the stratigraphy of Table 2.

The soil response is reported in Figure 5 for the input acceleration given by moment distribution called IBM_B. The synthetic accelerograms, at a depth of 30 m (i.e. conventional bedrock), is shown in Figure 5a. The soil response at the surface by 2-D SPEM simulation is reported in Figure 5b, for soil stratigraphy of site No. 3 (Table 2). The soil response at the surface by 1-D GEODIN simulation is reported in Figure 5c, also for soil stratigraphy of site No. 3 (Table 2). The 1-D simulation by GEODIN was made taking into account soil non-linearity given

by equations (1) and (2) for stiff soil, like that at San Nicola alla Rena Church site. Soil non-linearity for soft soil is taken into account later.

Comparing Figures 5b and 5c it is possible to see that using the same stratigraphy, similar soil responses at the surface are obtained by 2-D simulation ($a_{\max} = 3.36 \text{ m/s}^2$) and 1-D simulation ($a_{\max} = 3.44 \text{ m/s}^2$) for site No. 3.

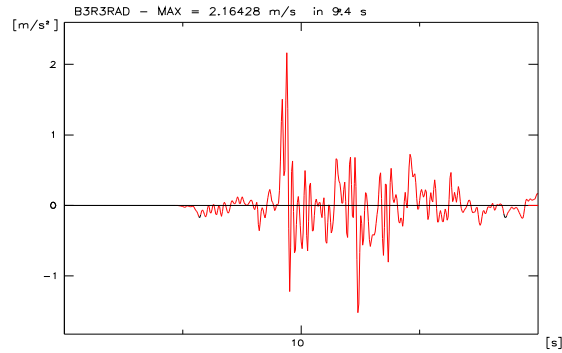
In Table 5 are reported the results obtained for input motion IBM_B for all seven sites considered, with the stratigraphy reported in Table 2 and with soil non-linearity given for stiff soil. In Table 6 are reported the results obtained for input motion IBM_B for the stratigraphies given by the boreholes of Table 3 related to the seven sites considered, for soil non-linearity given for stiff soil. If soil response by 1-D simulation is performed for site No. 7, for the more detailed soil stratigraphy given by boring No. 346 (Table 3), the soil response obtained by 1-D simulation ($a_{\max} = 4.12 \text{ m/s}^2$) is different from soil response obtained by 2-D simulation ($a_{\max} = 3.36 \text{ m/s}^2$) for soil stratigraphy for site No. 7 given by Table 2.

From a general point of view, results (Table 5) obtained by 2-D simulation and 1-D simulation agreed very well for soil stratigraphy given by Table 2. Results (Table 6) obtained by 1-D simulation are 38.5% higher than the simulation if we consider, as it is better to do when available, detailed soil stratigraphy given by boreholes of Table 3. In this case also the frequency becomes higher, because of the presence of some thin soil layer.

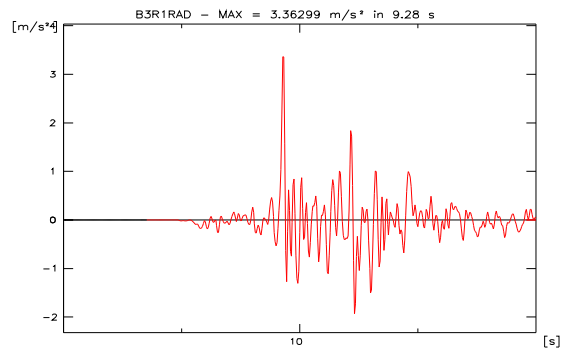
The 2-D simulation was evaluated for the four different seismic moment distribution of Figure 2 and for the seven sites of Figure 1. Artificial receivers were placed at different depths in each of the seven sites. In particular the synthetic accelerograms recorded by the artificial receivers placed at the surface and at a depth of about 30 m or deeper are analysed. The synthetic accelerograms recorded at about 30 m are considered as input motion for 1-D simulation. To analyse the effects of the position of the conventional bedrock, deeper synthetic accelerograms at depths ranging between 68 m and 74 m are considered as input motion for 1-D simulation. The results so far obtained by 1-D simulation at the surface are compared with those given by 2-D simulation considering the same input motion and the same V_s soil profile given by Table 2. This allow a comparison between 2-D and 1-D simulation results.

Table 4. Detailed evaluation of soil properties for borehole No. 408.

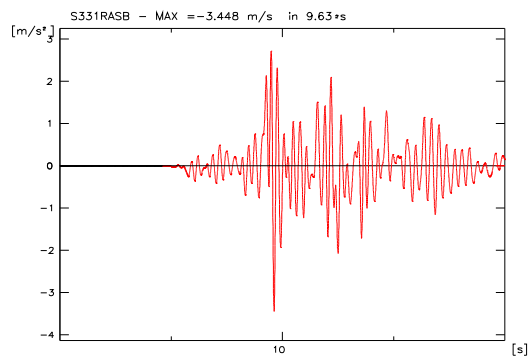
| Depth (m) | Soil formation | Soil mass (ρ) (KNs^2/m^4) | V_s (m/s) | G_0 (MPa) | D_{\min} (%) |
|-----------|----------------|--|-------------|-------------|----------------|
| 2.1 | Alf | 1.87 | 300 | 168.30 | 4.54 |
| 3.3 | Aa | 2.03 | 250 | 126.875 | 4.54 |
| 4 | Alf | 1.87 | 300 | 168.30 | 4.54 |
| 4.8 | Aa | 2.03 | 250 | 126.875 | 4.54 |
| 7.6 | Alf | 1.87 | 300 | 168.30 | 4.54 |
| 18 | Alg | 1.87 | 300 | 168.30 | 4.54 |



a) Synthetic accelerogram obtained by 2-D SPEM simulation for site No. 3 (radial component) and for receiver No. 3 at the depth of 31 m: $a_{\max} = 2.16 \text{ m/s}^2$.



b) Soil response at site No. 3 (Table 2) by 2-D simulation at surface: $a_{\max} = 3.36 \text{ m/s}^2$.



c) Soil response for site No. 3 (Table 2) by 1-D simulation: $a_{\max} = 3.44 \text{ m/s}^2$.

Figure 5. 2-D and 1-D soil response at site No. 3 for synthetic accelerograms IBM_B (radial component) as input, for soil non-linearity given by equation (2).

Table 5. Site response at surface for radial and tangential input motion IBM_B at different sites and different depths by 1-D GEODIN simulation and 2-D SPEM simulation: stratigraphy given by Table 2.

| | Depth (m) | Seismic input | Input Accel. (m/s ²) | 1-D Displac. (cm) | 1-D Velocity (m/s) | 1-D Accel. (m/s ²) | 2-D Accel. (m/s ²) |
|--------|--------------|------------------|--|-------------------------|--------------------------|--------------------------------------|--------------------------------------|
| SITE 1 | 34 | B1R3RAD | 1.76 | 0.74 | 0.12 | 2.44 | 2.81 |
| | 34 | B1R3TAN | 1.76 | 0.23 | 0.04 | 0.80 | 0.51 |
| SITE 2 | 32 | B2R3RAD | 1.66 | 0.91 | 0.15 | 3.17 | 3.00 |
| | 32 | B2R3TAN | 1.66 | 0.23 | 0.04 | 0.82 | 0.48 |
| SITE 3 | 31 | B3R3RAD | 2.16 | 0.86 | 0.18 | 3.44 | 3.36 |
| | 31 | B3R3TAN | 2.16 | 0.20 | 0.03 | 0.72 | 0.59 |
| SITE 4 | 27 | B4R3RAD | 1.68 | 0.74 | 0.11 | 3.47 | 3.30 |
| | 27 | B4R3TAN | 1.68 | 0.21 | 0.04 | 0.10 | 0.53 |
| SITE 4 | 70 | B4R5RAD | 1.89 | 3.34 | 0.30 | 3.12 | 3.30 |
| | 70 | B4R5TAN | 1.89 | 0.87 | 0.08 | 0.70 | 0.53 |
| SITE 5 | 32 | B5R3RAN | 1.90 | 0.91 | 0.16 | 3.00 | 3.38 |
| | 32 | B5R3TAN | 1.90 | 0.18 | 0.03 | 0.61 | 0.60 |
| SITE 5 | 74 | B5R5RAD | 1.53 | 2.54 | 0.19 | 2.28 | 3.38 |
| | 74 | B5R5TAN | 1.53 | 0.59 | 0.04 | 0.56 | 0.60 |
| SITE 6 | 31 | B6R3RAD | 1.91 | 0.74 | 0.01 | 2.82 | 2.97 |
| | 31 | B6R3TAN | 1.91 | 0.18 | 0.03 | 0.73 | 0.49 |
| SITE 6 | 72 | B6R5RAD | 1.74 | 2.96 | 0.23 | 2.56 | 2.97 |
| | 72 | B6R5TAN | 1.74 | 0.58 | 0.04 | 0.50 | 0.49 |
| SITE 7 | 30 | B7R3RAD | 1.25 | 0.58 | 0.07 | 2.08 | 2.40 |
| | 30 | B7R3TAN | 1.25 | 0.21 | 0.03 | 0.76 | 0.77 |
| SITE 7 | 68 | B7R5RAD | 1.07 | 1.87 | 0.12 | 1.81 | 2.40 |
| | 68 | B7R5TAN | 1.07 | 0.70 | 0.04 | 0.64 | 0.77 |

Table 6. Site response at surface for radial and tangential input motion IBM_B at different sites and different depths by 1-D GEODIN simulation and 2-D SPEM simulation: stratigraphy given by boreholes of Table 3.

| Borehole | Depth (m) | Seismic input | Input Accel. (m/s ²) | 1-D Displac. (cm) | 1-D Velocity (m/s) | 1-D Accel. (m/s ²) | 2-D Accel. (m/s ²) |
|----------|--------------|------------------|--|-------------------------|--------------------------|--------------------------------------|--------------------------------------|
| 1068 | 34 | B1R3RAD | 1.76 | 0.98 | 0.22 | 5.00 | 2.81 |
| | 34 | B1R3TAN | 1.76 | 0.23 | 0.05 | 1.15 | 0.51 |
| 1069 | 32 | B2R3RAD | 1.66 | 1.41 | 0.31 | 7.55 | 3.00 |
| | 32 | B2R3TAN | 1.66 | 0.28 | 0.06 | 1.52 | 0.48 |
| 408 | 31 | B3R3RAD | 2.16 | 0.91 | 0.19 | 4.12 | 3.36 |
| | 31 | B3R3TAN | 2.16 | 0.29 | 0.05 | 1.19 | 0.59 |
| 409 | 27 | B4R3RAD | 1.68 | 0.74 | 0.19 | 4.77 | 3.30 |
| | 27 | B4R3TAN | 1.68 | 0.23 | 0.51 | 1.45 | 0.53 |
| 409 | 70 | B4R5RAD | 1.89 | 4.83 | 0.66 | 8.08 | 3.30 |
| | 70 | B4R5TAN | 1.89 | 0.96 | 0.13 | 1.63 | 0.53 |
| 130 | 32 | B5R3RAN | 1.90 | 1.52 | 0.13 | 2.67 | 3.38 |
| | 32 | B5R3TAN | 1.90 | 0.48 | 0.06 | 0.81 | 0.60 |
| 130 | 74 | B5R5RAD | 1.53 | 4.06 | 0.44 | 4.60 | 3.38 |
| | 74 | B5R5TAN | 1.53 | 0.83 | 0.09 | 1.19 | 0.60 |
| 1427 | 31 | B6R3RAD | 1.91 | 2.07 | 0.23 | 4.26 | 2.97 |
| | 31 | B6R3TAN | 1.91 | 0.39 | 0.04 | 0.98 | 0.49 |
| 1427 | 72 | B6R5RAD | 1.74 | 3.68 | 0.44 | 5.50 | 2.97 |
| | 72 | B6R5TAN | 1.74 | 0.66 | 0.07 | 1.54 | 0.49 |
| 346DH | 30 | B7R3RAD | 1.25 | 0.48 | 0.14 | 3.87 | 2.40 |
| | 30 | B7R3TAN | 1.25 | 0.18 | 0.05 | 1.38 | 0.77 |
| 346 | 30 | B7R3RAD | 1.25 | 0.90 | 0.07 | 2.14 | 2.40 |
| | 30 | B7R3TAN | 1.25 | 0.34 | 0.04 | 0.48 | 0.77 |
| 346DH | 68 | B7R5RAD | 1.07 | 1.99 | 0.17 | 2.63 | 2.40 |
| | 68 | B7R5TAN | 1.07 | 0.93 | 0.09 | 1.01 | 0.77 |

By way of an example, in Figure 6 is reported the comparison between 2-D and 1-D soil response, for synthetic input accelerograms IBM_B (the most severe), for the same soil profile, given by Table 2. Soil non-linearity is given by equations (1) and (2) for stiff soil like that of the San Nicola alla Rena Church site. From Figure 6 and Table 5, it is possible to see that 2-D and 1-D simulations show very similar results (2-D results are higher than 1-D results by only 6%) and very close site amplification (1.71 with 2-D simulation and 1.60 with 1-D simulation).

By way of an example in Figure 7 is reported the comparison between 2-D and 1-D soil response for synthetic input accelerograms IBM_B (the most severe) for different soil profiles, given by Table 2 in 2-D simulation and by the boreholes of Table 3 for 1-D simulation. The soil non-linearity is given again by equations (1) and (2), for stiff soil like that of the San Nicola alla Rena Church site. From Figure 7 and Table 6 it is possible to see that 2-D and 1-D simulations show different results (2-D results are lower than 1-D results by 38.5%) and different site amplifications of 1.72 with 2-D simulation and 2.80 with 1-D simulation.

From Figures 6 and 7 it can be argued that the most uncertainties for the Catania area are not linked with 2-D or 1-D simulation, but with the properties of the upper part of the soil profile. A depth of 30 m, suggested by Eurocode [1] or even a deeper depth up to 74 m have been considered. A detailed soil profile is usually evaluated by boreholes and by estimation of shear wave velocity. When *in situ* tests are available empirical relationships to link shear wave velocity to test sites or laboratory tests in the static field are used. The average uncertainty, linked with the conventional bedrock position, is of 12% (Figure 6) and 18% (Figure 7), moving from a depth of about 30 m to a depth of about 70 m.

From Table 6 it is possible to see that in one case a detailed soil profile was evaluated very accurately by down-hole tests. The use of this profile, instead of an estimated one, makes some difference to the results. The uncertainty on the a_{max} is about of 44% (see Table 6).

Figure 8 shows the comparison of 2-D and 1-D soil responses for the input synthetic accelerograms IBM_B, for different soil profile, considering soil non-linearity given by the equations (1) and (2), for soft soil like that of the via Stellata site. From Figure 8a it is possible to see that 2-D and 1-D simulations show different results (2-D results are higher than 1-D results by 31.50%) and different site amplifications of 1.79 with 2-D simulation and 1.22 with 1-D simulation. From Figure 8b, it is possible to see that 2-D and 1-D simulations show very similar results (2-D results are higher than 1-D results by only 3%) and very close site amplification (1.92 with 2-D simulation and 1.86 with 1-D simulation).

Comparing the results shown in Figure 6a with those of Figure 8a, obtained for the same input accelerograms IBM_B and the same stratigraphy given by Table 2, it is possible to evaluate the uncertainty linked with soil non-linearity. In fact if we consider stiff soil the average soil amplification is 1.71 with 2-D simulation and 1.60 with 1-D simulation, while if we consider soft soil, the soil amplification is 1.92 with 2-D simulation and 1.86 with 1-D simulation.

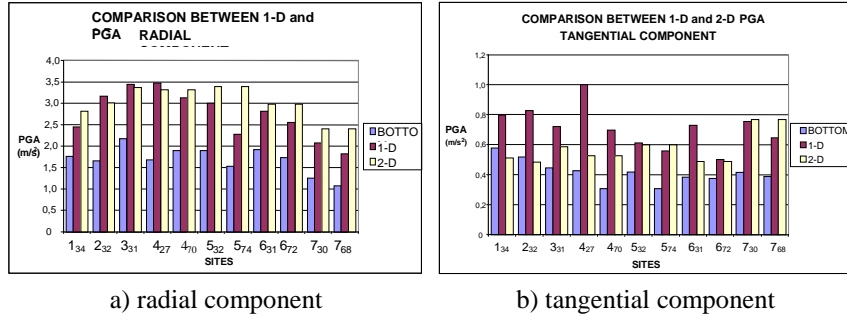


Figure 6. Comparison between 2-D and 1-D soil response for synthetic input accelerograms IBM_B at bottom, for stratigraphy given by Table 2 and for stiff soil (see Table 5).

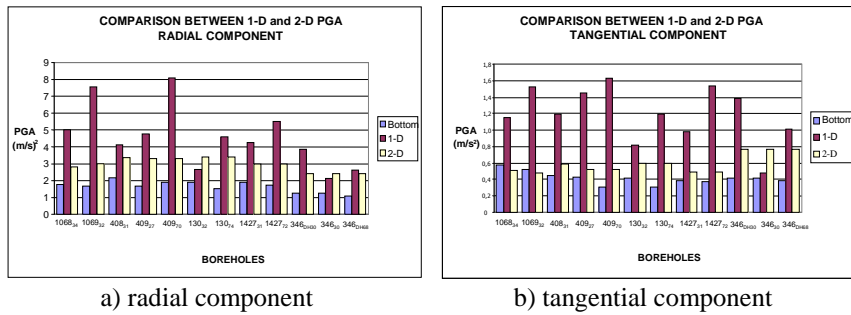


Figure 7. Comparison between 2-D and 1-D soil response for synthetic input accelerograms IBM_B at bottom, for stratigraphy given by boreholes and for stiff soil (see Table 6).

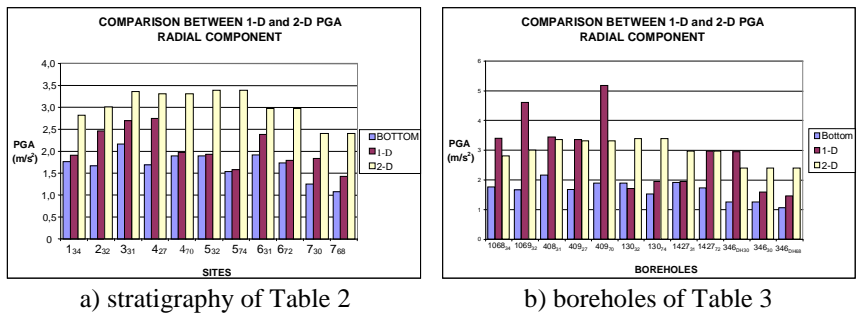


Figure 8. Comparison between 2-D and 1-D soil response for synthetic input accelerograms IBM_B at bottom, radial component, for soft soil.

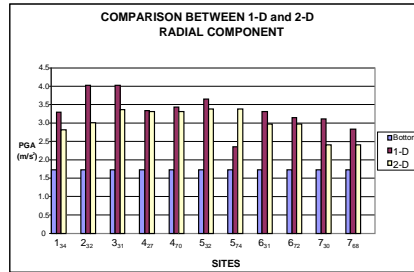
Comparing the results shown in Figure 7a with those of Figure 8b, obtained for the same input accelerograms IBM_B and the same stratigraphy given by the boreholes of Table 3, it is possible to evaluate again the uncertainty linked with soil non-linearity. In fact if we consider stiff soil the average soil amplification is 1.79 with 2-D simulation and 1.22 with 1-D simulation, while if we consider soft soil, the soil amplification is 1.92 with 2-D simulation and 1.86 with 1-D simulation. It can be argued that the uncertainty linked with soil non-linearity for the Catania area is more relevant than 2-D or 1-D simulation effects. This could be due to the fact that Catania soil shows many asperities but not hill or ridge effects.

1-D simulation has been performed not only for synthetic input 2-D accelerograms, but also for input scaled accelerograms recorded during the December 13, 1990 eastern Sicily earthquake ($M=5.7$). The results obtained for the soil stratigraphies given by Table 2 are reported in Figures 9-11. In Figure 10 is reported the case of the not scaled Catania E-W component input motion. In Figure 11 is reported the case of Catania N-S component input motion scaled to the maximum value of acceleration given by the 2-D synthetic accelerograms recorded by artificial receiver at a given depth. In Figure 11 is reported the case of Sortino E-W component input motion scaled to the maximum value of acceleration given by the 2-D synthetic accelerograms recorded by artificial receiver at a given depth. In Figures 9-11 the depth of the conventional bedrock is reported as subscript for each of the seven sites considered. From a general point of view Figures 9-11 show that the results 2-D and 1-D simulation are in good agreement for firm soil (Figures 9a, 10a and 11a) while for soft soil 2-D simulation shows higher peak ground acceleration than 1-D simulation (Figures 9b, 10b and 11b), because 2-D simulation neglects the soil non-linearity.

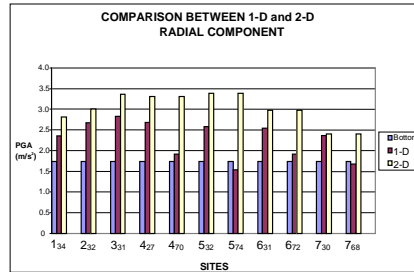
1-D simulations have been also performed, using scaled input accelerograms, for the soil stratigraphies given by boreholes of Table 3. From a general point of view, in this case 2-D and 1-D simulations show different results for stiff soil (2-D results are lower than 1-D), while they agree well for soft soil. This could be explained by the fact that the 1-D simulation for stiff soil gives higher site amplification related to the presence of more soil layers with thinner thickness than 2-D simulation. When we consider soft soil, 2-D simulation gives very higher values of site amplification because it neglects soil non-linearity, which is considered by 1-D simulation.

4 Conclusions

A comparison between soil responses at the surface given by the 2-D Spectral Element Method and 1-D simulation is presented and discussed. 1-D simulation is performed using as input motion at the conventional bedrock synthetic 2-D accelerograms and scaled recorded accelerograms. In particular the effects on site amplification due to seismic input, conventional bedrock position, shear wave soil profile and soil non-linearity are analysed and discussed. The uncertainties linked with these effects are also referred to.

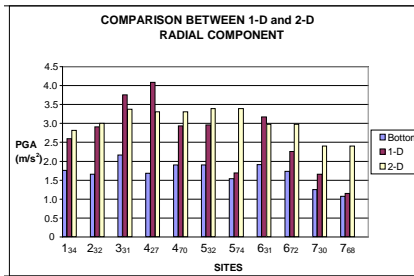


a) firm soil

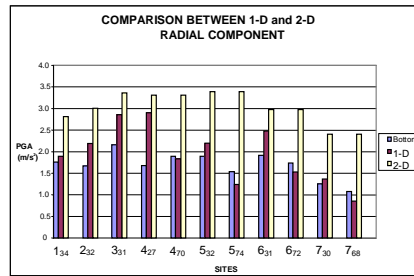


b) soft soil

Figure 9. Comparison between 2-D and 1-D soil response for Catania 13.12.1990 E-W input accelerograms at bottom, for stratigraphy given by Table 2.

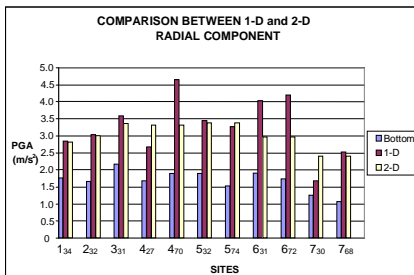


a) firm soil

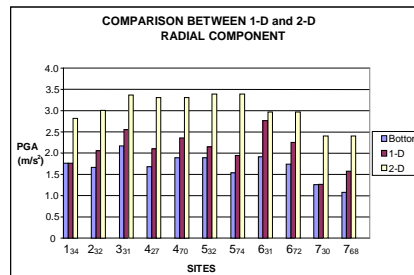


b) soft soil

Figure 10. Comparison between 2-D and 1-D soil response for Catania 13.12.1990 N-S scaled input accelerograms at bottom, for stratigraphy given by Table 2.



a) firm soil



b) soft soil

Figure 11. Comparison between 2-D and 1-D soil response for Sortino 13.12.1990 E-W scaled input accelerograms at bottom, for stratigraphy given by Table 2.

References

- [1] Eurocode n. 8, 2002. Design of structures Earthquake Resistance. Part 1: General rules, seismic actions and rules for buildings, May 2002.
- [2] Seriani, G. and Priolo, E., 1994. Spectral element method for acoustic wave simulation in heterogeneous Media. *Finite Elements in Analysis and Design*, 16, 337-348.
- [3] Priolo, E., 1999. 2-D spectral element simulations of destructive ground shaking in Catania (Italy). *J. of Seismology*, 3(3), 289-309.
- [4] Priolo, E., 2001. Earthquake ground motion simulation through the 2-D spectral element method. *J. Comp. Acoustics*, 9 (4).
- [5] Postpischl, D., 1985. Atlas of Isoseismal Maps of Italian Earthquakes. Editor Postpischl. *CNR-Progetto Finalizzato Geodinamica*, Rome, 164 pp.
- [6] Heaton, H., 1990. Evidence for and implications of self-healing pulses of slip in earthquake rupture. *Physics of Earth and Planetary Interiors*, 64, 1-20.
- [7] Wells, D.L. and Coppersmith, K.J., 1994. New empirical relationships among magnitude, rupture length, rupture width, rupture area, and surface displacement, *Bull. Seism. Soc. Am.*, 84, 974-1002.
- [8] Sommerville, P., Irikura, K., Graves, R., Sawada, S., Wald, D., Abrahamson, N., Iwasaki, Y., Kagawa, T., Smith, N. and Kowada, A., 1999. Characterizing crustal earthquake slip models for the prediction of strong ground motion. *Seism. Res. Lett.*, 70, 59-80.
- [9] Frenna, S.M. and Maugeri, M., 1995. GEODIN: a Computer Code for Seismic Soil Response. *Proceedings of the 9th Italian Conference on Computational Mechanics*. Catania, Italy, 20-22 June, pp. 145-148.
- [10] Maugeri, M. and Frenna, S.M., 1987. Simplified hysteretic model for non-linear soil response. *Proc. 3rd Nat. Conference: "L'Ingegneria sismica in Italia"*, Rome, September 30-October 2, 1987, Vol. II, pp. 269-288 (in Italian).
- [11] Maugeri, M., Carrubba, P. and Frenna, S.M., 1988. Vibration mode and predominant frequency of heterogeneous soil. *Italian Geotechnical Journal*, Vol. XXII, n. 3, pp. 163-171.
- [12] Rovelli, A., Boschi, E., Coco, M., Di Bona, M., Berardi, R. and Longhi, G., 1991. Il terremoto del 13/12/1990 nella Sicilia Orientale: analisi dei dati accelerometrici. Istituto Nazionale di Geofisica, pubbl. n. 537, pp. 85-101.
- [13] Maugeri, M. and Cavallaro, A., 2000. Non linear soil behaviour of Catania clays. In: *The Catania Project: Earthquake Damage Scenarios for a high risk area in the Mediterranean*. Editors: Faccioli and Pessina. CNR-GNDT-Roma 2000, pp. 38-41.
- [14] Cavallaro, A., Grasso, S. and Maugeri, M., 2001. A dynamic geotechnical characterisation of soil at Saint Nicola alla Rena Church site damaged by the south eastern Sicily earthquake of 13 December 1990. *XV Int. Conf. on Soil Mechanics and Geotechnical Engineering*, Istanbul, Turkey, 24 August 2001.